Advances in Nano Research, *Vol. 7 No. 1 (2019) 39-49*
DOI: https://doi.org/10.12989/anr.2019.7.1.039

Characterization and behaviors of single walled carbon nanotube by equivalent-continuum mechanics approach

Mohamed A. Eltaher [*1,2], Talaal A. Almalki [1], Khaled I.E. Ahmed [1,3] and Khalid H. Almitani [1]

[1] *Mechanical Engineering Dept., Faculty of Engineering, King Abdulaziz University, P.O. Box 80204, Jeddah, Saudi Arabia*
[2] *Mechanical Design & Production Dept., Faculty of Engineering, Zagazig University, P.O. Box 44519, Zagazig, Egypt*
[3] *Mechanical Engineering Department, Faculty of Engineering, Assiut University, P.O. Box 71516, Assiut, Egypt*

(*Received November 25, 2018, Revised January 12, 2019, Accepted January 14, 2019*)

Abstract. This paper focuses on two main objectives. The first one is to exploit an energy equivalent model and finite element method to evaluate the equivalent Young's modulus of single walled carbon nanotubes (SWCNTs) at any orientation angle by using tensile test. The calculated Young's modulus is validated with published experimental results. The second target is to exploit the finite element simulation to investigate mechanical buckling and natural frequencies of SWCNTs. Energy equivalent model is presented to describe the atomic bonding interactions and their chemical energy with mechanical structural energies. A Program of Nanotube modeler is used to generate a geometry of SWCNTs structure by defining its chirality angle, overall length of nanotube and bond length between two adjacent nodes. SWCNTs are simulated as a frame like structure; the bonds between each two neighboring atoms are treated as isotropic beam members with a uniform circular cross section. Carbon bonds is simulated as a beam and the atoms as nodes. A finite element model using 3D beam elements is built under the environment of ANSYS MAPDL environment to simulate a tensile test and characterize equivalent Young's modulus of whole CNT structure. Numerical results are presented to show critical buckling loads, axial and transverse natural frequencies of SWCNTs with different orientation angles and lengths. The understanding of mechanical behaviors of CNTs are essential in developing such structures due to their great potential in wide range of engineering applications.

Keywords: numerical characterization; equivalent Young's modulus of SWCNT; buckling and free vibration; beam structure; finite element ANSYS

1. Introduction

A nanotube is a tube that has a diameter in a range of tens of billionth meter, and its abbreviation is NT. There are different types of nanotubes such as carbon nanotubes (CNTs), silicon nanotubes, DNA and the membrane nanotube. Iijima (1991) discovered CNT structure, which is defined as a long and thin fullerene structure with tubular walls made of hexagonal carbon cells. CNTs have extraordinary properties rather than conventional materials, so they have received widespread interest of researchers from many disciplines (i.e., material science, engineering, chemistry, and physics) and are applied in wide range of applications (i.e., nanoelectronics, nano-sensors, solar cell, medical tools and nanodevices), Benguediab *et al*. (2014). Until now, CNTs are considered as the strongest and most resilient material ever known, Eltaher and Agwa (2016).

To understand the mechanical performance of CNTs, theoretical approaches such as; atomistic modeling and continuum mechanics are exploited. Atomistic modeling methods such as quantum mechanics (QM) and molecular dynamic (MD) simulations are frequently used to investigate fracture behavior of CNTs, Haile (1992). Li and Chou (2003) developed atomistic based FE models that bridge the MMs and structural mechanics, using harmonic potential energy functions to investigate the elastic properties of SWCNTs. Baykasoglu *et al*. (2013) presented nonlinear fracture models including one- and two-atom vacancy defected SWCNTs by using the molecular mechanics. Eberhardt and Wallmersperger (2015) presented a modified molecular structural mechanics model to determine elastic properties of CNTs. It is noted that, elastic constants are found to be dependent on the chirality as well as on the carbon nanotube diameter. Gajbhiye and Singh (2015) studied vibration characteristics of open- and capped-end SWCNTs using multi-scale technique incorporating Tersoff–Brenner potential. Ghadyani *et al*. (2016) developed an algorithm based on a numerical finite element analysis, to relate the physical geometry to the elastic properties of asymmetric SWCNTs. Ghadyani *et al*. (2017) exploited previous algorithm to illustrate angle dependence of the shear behavior of asymmetric CNTs. Alessi *et al*. (2017) proposed a finite-deformation lattice model for CNTs that assigned to changes in bond lengths, bond angles, and dihedral angles, while atomic interactions are governed by a reactive empirical bond-order potential. Esbati and Irani (2018) developed procedure for evaluating CNTs' probabilistic fracture properties and structural reliability using stochastic finite element methods. It is demonstrated that, the defects out of critical section have an

*Corresponding author, Professor,
E-mail: meltaher@kau.edu.sa; mmeltaher@zu.edu.eg

ISSN: 2287-237X (Print), 2287-2388 (Online)

unavoidable effect on Young's modulus and ultimate strain, however, they have an insignificant effect on ultimate stress. Shahabodini *et al*. (2018) developed a numerical approach for the multiscale analysis of vibrations of SWCNTs by using higher order Cauchy-Born rule kinematics membrane.

Although MD can be applied to larger systems, it is still limited to simulating about 106–108 atoms on a too-short time scale, Lu and Hu (2010). Therefore, the simulation of larger systems or longer times must currently be left to continuum methods, Narendar and Gopalakrishnan (2009). Lee and Lee (2012) presented modal analysis of SWCNTs and nanocones (SWCNCs) using a finite element method (FEM) with ANSYS. Caruntu and Luo (2014) investigated frequency response of electro statically actuated CNT cantilever beam over a parallel ground plate including van der Waals, and damping. Akgöz and Civalek (2016) studied static bending of single-walled carbon nanotubes (SWCNTs) embedded in an elastic medium on the basis of higher-order sheared formation beam models in conjunction with modified strain gradient theory. Eltaher and Agwa (2016) developed modified continuum mechanics model to investigate a vibration of a pretensioned CNTs carrying a concentrated mass as a mass sensor. Eltaher *et al*. (2016a) investigated the effects of both size-dependency and material-dependency on the nonlinear static behavior of CNTs by using nonlocal elasticity and energy-equivalent model. Eltaher *et al*. (2016b) developed a simplified nonlocal finite element model to investigate the potential application of CNTs as a nanomechanical mass sensor by using nonlocal differential elasticity of Eringen. Eltaher *et al*. (2016c) studied analytically static stability of nonlocal nano-thin-structure using higher-order beam theories. Zuberi and Esat (2016) evaluated the effects of tube size and chirality on the mechanical properties of SECNTs through equivalent-continuum modeling. Genoese *et al*. (2017) presented the energetic differences between structural models and molecular mechanics model through exact discrete homogenization procedures, and reparametrized Morse potential. She *et al*. (2017a) investigated the size-dependent thermal buckling and post-buckling behavior of nanotubes made of functionally graded materials (FGMs) with porosities by using a refined beam theory. She *et al*. (2017b) studied nonlinear bending, thermal buckling and post-buckling analysis for functionally graded materials tubes with two clamped ends by using a refined beam theory. Eltaher *et al*. (2018a) developed a modified continuum model to investigate the vibration behavior of CNTs by using energy equivalent model and modified couple stress theory. Emam *et al*. (2018) exploited modified continuum mechanics models to investigate the post-buckling and free vibration response of geometrically imperfect multilayer nanostructures. She *et al*. (2018a) analyzed the nonlinear bending and vibrational characteristics of porous tubes within the framework of the nonlocal strain gradient theory. Ebrahimi and Mahmoodi (2018) studied the thermal loading effect on free vibration characteristics of carbon nanotubes (CNTs) with multiple cracks. Nanotube in the framework of Euler-Bernoulli beam theory and size effect is employed by the nonlocal elasticity of Eringen. Kumar (2018) investigated mechanical vibration of double-walled carbon nanotubes with inter-tube Van der waals forces. She *et al*. (2018b) studied the vibration behaviors of porous nanotubes by using the nonlocal strain gradient theory in conjunction with a refined beam model. Eltaher *et al*. (2018 b, c) studied analytically bending, buckling and resonance frequencies of size dependent perforated modified continuum model of nanobeam. Vila *et al*. (2018) studied coupled axial-transverse nonlinear vibrations of one-dimensional structured solids by application of the so-called Inertia Gradient Nonlinear continuum model. Yuan and Wang (2018) explored the radial deformation and related energy variations of SWCNTs attached to solid substrates by adopting the classical molecular dynamics (MD) simulations and continuum analysis. Eltaher *et al*. (2019) presented a novel numerical procedure to predict nonlinear buckling and postbuckling stability of imperfect clamped–clamped SWCNT surrounded by nonlinear elastic foundation. She *et al*. (2019) described the stiffness enhancement and stiffness reduction effects by the nonlocal strain gradient theory to study the nonlinear bending behavior of porous functionally graded (FG) curved nanotubes.

From the literature review and to the best of the authors' knowledge, no attempts have been observed to characterize the Mechanical behavior of SWCNT including length scale-size dependency by using Finite element method. So, Mechanical characterization of SWCNT using finite element analysis is the main goal of this study. Through this study, the bond between two atoms is modeled as beam structure. The energy equivalent model is proposed to find the equivalent mechanical energy of the structure with that in chemical bonding of atoms. Nanotube modeler is used to generate a geometry of CNTs that is impeded to the finite element model which is solved by ANSYS MAPDL to study the vibration behavior of its structure. Equivalent Young's modulus of SWCNT with various chiral angle and length is evaluated. Critical buckling loads and their mode shapes are presented. The natural frequencies of zigzag, armchair and chiral SWCNT are studied and their associated modes are illustrated.

The following paper is organized as follows; geometrical properties and orientations of SWCNT are presented in detail in Section 2. Mathematical formulation is illustrated in Section 3. Section 4 is devoted to validating the finite element model and then to find the equivalent Young's modulus of SWCNTs. Section 5 discussed the static buckling of different orientations and length of SWCNTs. Free vibration and natural frequencies are evaluated and discussed in Section 6. The main contribution and investigations are drawn in Section 7.

2. Geometrical properties of SWCNTs

Carbon nanotube, which is a layer of graphene sheet wrapped into cylindrical shape with a diameter about one nanometer and a length up to many micrometers, is controlled by orientation of the chiral angle and the carbon

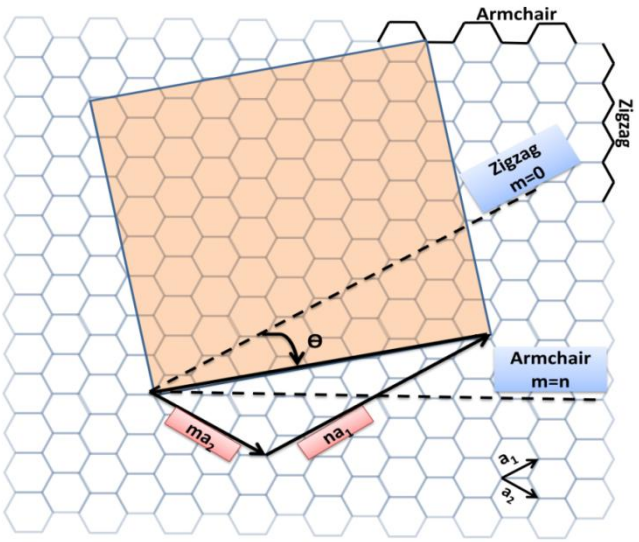

Fig. 1 Schematic of the hexagonal lattice of graphene sheet including definition of basic structural parameters

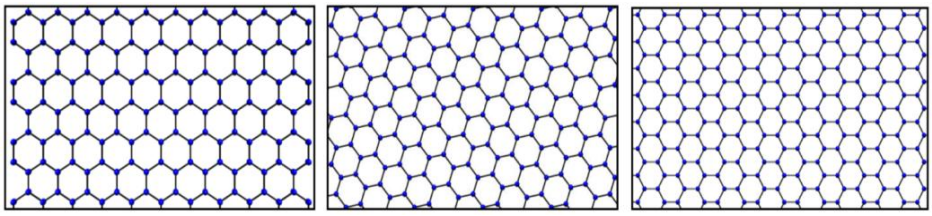

(a) Graphene sheets before rolling

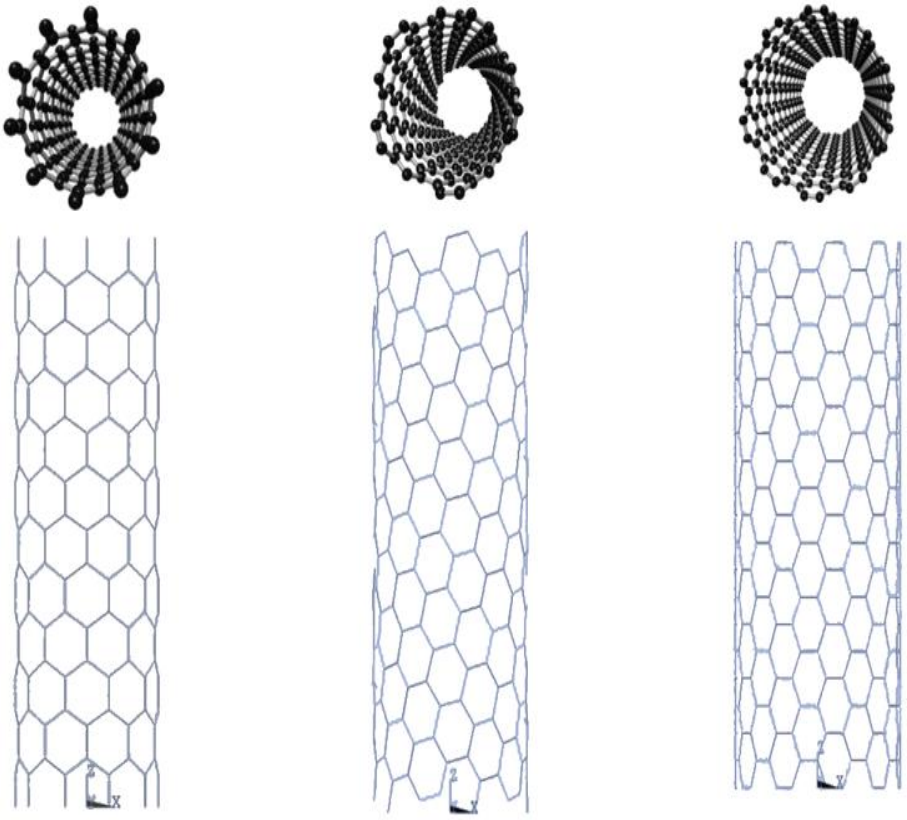

Zigzag Chiral Armchair

(b) Graphene sheets after rolling

Fig. 2 Three possible structure orientations of SWCNTs

diameter. The chiral vector is employed to describe the chiral angle, which can be described as, Eltaher *et al.* (2016a)

$$\vec{C}_h = n\vec{a}_1 + m\vec{a}_2 \tag{1}$$

where $\vec{a}_1$ and $\vec{a}_2$ are the unit vectors, and (n, m) is integer pair specifies the structure orientation of CNTs as shown in Fig. 1. The lattice vectors in the x, y coordinates can be depicted by

$$\vec{a}_1 = \left(\frac{\sqrt{3}a}{2}, \frac{a}{2}\right) \qquad \vec{a}_2 = \left(\frac{\sqrt{3}a}{2}, -\frac{a}{2}\right) \tag{2}$$

in which, the lattice constant, $a = \sqrt{3}a_{c-c} = 2.46\,A^0$ and $a_{c-c} = 1.42A^0$ is the bond length. When n and m are equal, CNTs are called armchair; when m is equal to zero, CNTs are known as zigzag. Otherwise, they are called chiral. Fig. 2 shows the three possible orientations of CNTs structure. Fig. 2(a) represents the orientation of graphene sheets before rolling, whereas, Fig. 2(b) shows the structure of grapheme sheet after rolling to NTs.

The diameter (d_t) and chiral angle (θ) which is the angle between the chiral vectors and lattice vector, can be calculated by the following equations, Eltaher and Agwa (2016)

$$d_t = a\sqrt{n^2 + m^2 + nm} \tag{3}$$

$$\theta = \cos^{-1}\left(\frac{2n+m}{\sqrt{n^2+m^2+nm}}\right) \tag{4}$$

In case of Zigzag and armchair orientations, the diameter of nanotube can be calculated by $d_t = \frac{\sqrt{3}na}{\pi}$, and $d_t = \frac{3na}{\pi}$, respectively. Note the chiral angle in zigzag = 0, while the chiral angle in the armchair = 30 after which, any configuration at any angle will be a repetition for another configuration at smaller angle.

3. Problem formulation

To establish a linkage between the microscopic chemistry and the macroscopic mechanics, covalent bonds between carbon atoms is represented by a force filed as a function of bond lengths and bond angles. The force filed can be represented by a potential energy as (Rappé *et al.* 1992)

$$PE = PE_L + PE_\theta + PE_T + PE_\omega \tag{5}$$

where PE_L, PE_θ, PE_T, and PE_ω are bond stretching, angle variation, torsion and inversion (out of plane) energies. These interactions are shown in Fig. 3.

When SWCNTs subjected to tension and bending loading in two-dimensional loading, bond stretching and angle energies are the most significant and the other energies can be neglected. Therefore, Eq. (5) can be simplified as, Wu *et al.* (2006), Shokrieh and Rafiee (2010), and Eltaher and Agwa (2016)

$$PE = PE_L + PE_\theta = \frac{1}{2}\sum_i K_i(dR_i)^2 + \frac{1}{2}\sum_j C_i(d\theta_i)^2 \tag{6}$$

Where K_i is the stretching constant, dR_i is the elongation of the bond i, C_i is the angle variance constant, and $d\theta_i$ is the variance of bond angle i. By assuming that, the chemical covalent bond can be represented by beam structure. So, based on continuum mechanics, the total energy stored in beam element can be composed mainly from tension and bending deformations. Hence, the total energy of a beam can be described by the following equation

$$U = U_T + U_b = \frac{1}{2}\frac{EA}{L}(\Delta L)^2 + \frac{1}{2}\frac{EI}{L}(2\alpha)^2 \tag{7}$$

where E is the Young's modulus, L is the beam length, A is the beam cross sectional area, I is the beam area moment of inertia, ΔL is stretching length, and 2α is rotation angle due to bending moment. By equating chemical energy in single atom-atom bond described in Eq. (6) with Eq. (7) of total energy of the beam, it can be concluded that

$$K_i = \frac{EA}{L} \quad \text{and} \quad C_i = \frac{EI}{L} \tag{8}$$

Since, the bond is circular cross sectional, the geometrical parameters of the bond can be calculated by

$$A = \frac{\pi d^2}{4} \quad \text{and} \quad I = \frac{\pi d^4}{64} \tag{9}$$

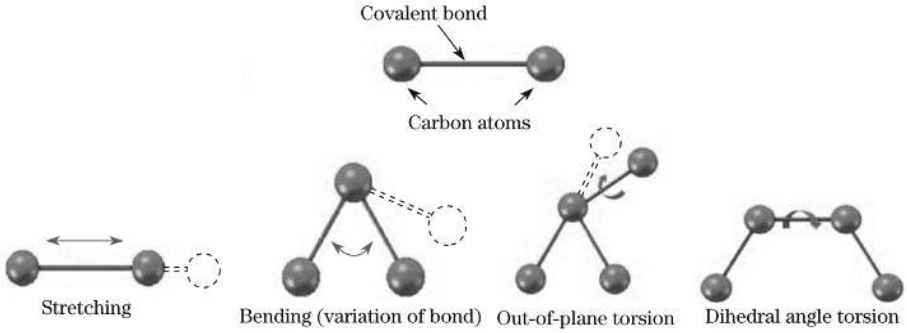

Fig. 3 Total potential energy store in single atom-atom bond

Table 1 FE Input properties and obtained Young's Moduli

Test case	Case 1	Case 2
Reference	Krishnan *et al*. (1998)	Awang *et al*. (2015)
Young's modulus of each bond	5.49E12 Pa	E = 5.49E12 Pa
Overall CNT length is L	234 Å	10 Å
Mean diameter of tube is d	11.2 Å	7.834 Å
Mean tube thickness is t	3.4 Å	3.4 Å
Poisson's ratio is υ	0.3	0.3
Equivalent Young's modulus (FE)	0.72 TPa	0.749 TPa
Equivalent Young's modulus (Exp.)	0.72-1.32 TPa	0.749 TPa

Substitute Eq. (9) into Eq. (8), the bonding diameter and Young's modulus of equivalent beam element can be described by

$$d = 4\sqrt{\frac{C_i}{K_i}} \quad \text{and} \quad E = \frac{(K_i)^2}{4\pi C_i} \tag{10}$$

4. Static analysis of SWCNTs

Through this section, the determination of equivalent Young's modulus of SWCNTs is presented by using finite element model that is solved by ANSYS MAPDL program. Nanotube modeler is exploited to generate the coordinates of carbon atoms and atomic bond interconnection between two adjacent atoms. Fig. 4 shows the finite element model of a 10A CNT with fixed-free ends. The atoms coordinate, and its bonding connectivity are translated to finite elements nodes with 3D beam element connectivity. The obtained results are validated with both experimental and numerical published works. Then, the influence of the length of CNT and its orientations on the equivalent Young's modulus are presented.

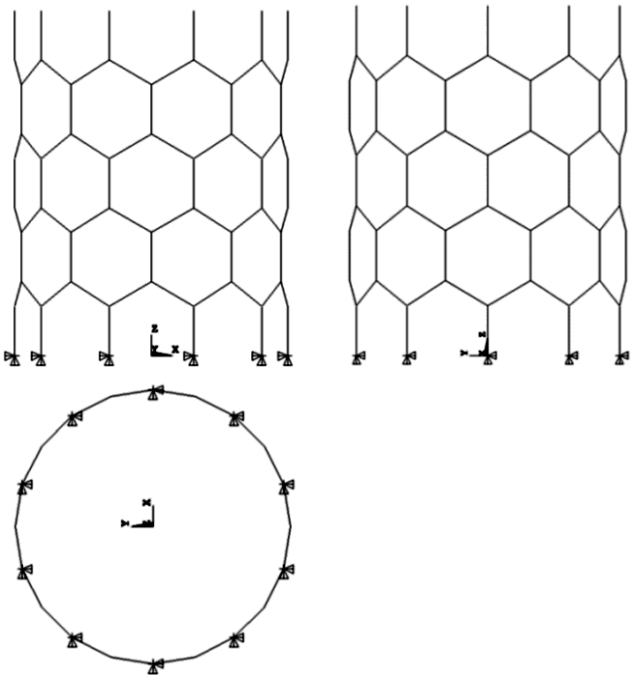

Fig. 4 Finite element model of 10A CNT with fixed-free ends

4.1 Characterization of Young's Modulus

The SWCNT is modeled using finite element model with 3D beam elements. The nodes represent the atom and the beams represent the bonding force as explained by Eqs. (6)-(10). The finite element model is verified by two previously published measurements; Krishnan *et al*. (1998) and Awang *et al*. (2015). A fixed-free CNT is proposed with the properties listed in Table 1. The force reaction at fixed end is evaluated and the equivalent Young's modulus of CNT is calculated by

$$E_{eq} = \frac{FL}{\pi d\, t\Delta L} \tag{11}$$

Where;

E_{eq} is the equivalent Young's Modulus

F is the obtained reaction force due to unit displacement L

L is the overall CNT length

d is the mean diameter of the tube

t is the mean tube thickness

The input data and the comparisons of achieved results from both verification cases are presented in Table 1.

4.2 Influence of CNTs length and orientations on Young's modulus

Fixed-free carbon nanotubes at different orientations [zigzag (10,0), chiral (10,5) and armchair (10,10)] and lengths ranging from 10 Å to 100 Å are tested under a prescribed displacements DL with 0.02 Å by using the finite element model. The finite element model examines full closed nano cells, which results in slightly smaller length than the starting defined length L as presented in Table 2. The variation of equivalent Young's modulus with NT lengths at a specific orientation are illustrated in **Table 2 and Fig 5**. As shown, the equivalent Young's modulus of CNT(10,5) orientation is most significant for a length variation rather other orientations. It decreases form 0.78 TPa at a length of 10 Å to 0.72TPa at a length of 100Å. As illustrated in Fig. 5, increasing the tube length tends to decrease the equivalent modulus for CNT (10, 0) and CNT (10,5). However, in case of CNT (10, 10) a little bit

Table 2 Effect of NT lengths on the equivalent Young's modulus

Type	Diameter	L (Length)	L (FE)	E_{eq} (TPa)
CNT (10,0)	7.834	10	9.947	0.7496
		20	19.22	0.7113
		30	29.841	0.7061
		40	39.788	0.7164
		50	49.0245	0.7054
		60	59.682	0.7061
		70	69.629	0.7104
		80	80.2963	0.7103
		90	89.523	0.7049
		100	100.181	0.7049
CNT (10,5)	10.364	10	10.2047	0.7773
		20	19.8937	0.7400
		30	29.8084	0.7315
		40	39.95	0.7228
		50	49.9491	0.7224
		60	58.8128	0.7060
		70	70.0899	0.7186
		80	78.95	0.7068
		90	90.2307	0.7165
		100	99.8983	0.7158
CNT (10,10)	13.57	10	9.845	0.7024
		20	19.69	0.7128
		30	29.5349	0.7076
		40	39.38	0.7115
		50	49.2249	0.7086
		60	59.07	0.7110
		70	70.1455	0.7091
		80	79.9932	0.7108
		90	89.8354	0.7093
		100	99.6804	0.7094

increasing of Young's modulus by increasing a tube length. The chiral orientation of CNT (10, 5) has the highest elasticity rather than Zigzag CNT (10, 0) and armchair CNT (10, 10) orientations. It is worth noting that the nodes at the ends of the Chiral tube CNT (10, 10) are not laying in the same plane due to full cell concept and chiral angle. This uneven orientation significantly affects the equivalent Young's modulus at short tube lengths rather than long tube lengths. This explains the different behavior of CNT (10,10) from the other two configurations as shown in Fig. 5.

5. Static buckling stability

Through this section, static stability of elastic carbon nanotube with different orientation and different tube length will be investigated. The first nine buckling loads of fixed-free zigzag (10, 0), Chiral (10, 5) and armchair (10, 10) which have the same diameter are presented in **Table 3** and **Fig. 6**. Axial force is applied at free end with a value of 3^{10} N, and Eigen buckling solution module is used to calculate the critical buckling load. It is noted that the armchair nanotube has the highest buckling rather than chiral and zigzag orientations as shown in **Fig. 6**. It is also noted that, there are repeated modes due to the symmetric configuration about the tube length axis. Complete buckling modes of zigzag, chiral and armchair nanotube structures at different orientations are presented in **Appendix A**.

The effect of tube length on the first nine critical buckling loads of Zigzag (10, 0), chiral (10, 5) and armchair (10, 10) are presented in Figs. 7-9, respectively. From previous figs, it is noticed that, the buckling load is decreased by increasing tube length, which is consistent with fundamental of mechanics. The effect of beam length is most significant on higher modes of buckling rather than lower modes, especially for zigzag (10, 0) shown in **Fig. 7**. It is also noted that, the length may change the number of repeated modes. For example, 5^{th} and 6^{th} modes of zigzag (10, 0) with a length of 100 Å are repeated modes, however, 5 modes are repeated (5^{th}, 6^{th}, 7^{th}, 8^{th} and 9^{th}) for different length at 70 Å. Therefore, the buckling loads and mode shape are significant for tube length and orientations. This analysis may use to select the proper directional position of sensing of Nano-sensor manufacture by carbon nanotube.

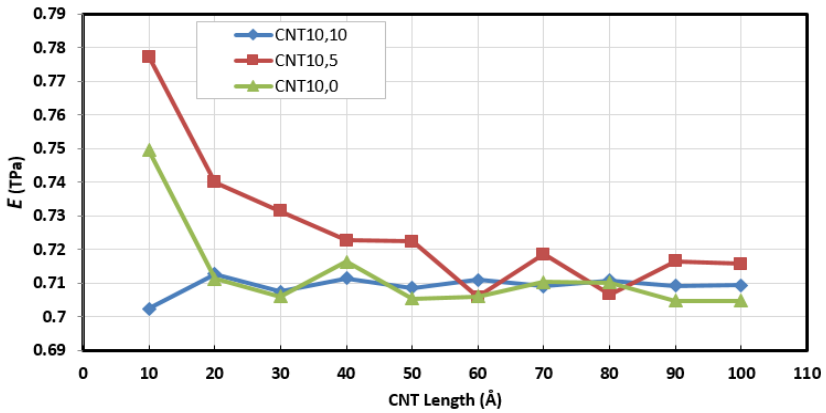

Fig. 5 Effect of NT length on the equivalent Young's modulus

Table 3 Buckling modes and force (10^{-8} N), when L_{FE} = 100, F_{FE} = 3^{10} N

Mode	1st	2nd	3rd	4th	5th	6th	7th	8th	9th
CNT (10,0)	0.110808	0.110809	0.930668	0.930677	2.27887	2.278	3.78272	3.78278	5.14434
CNT (10,5)	0.262751	0.26277	2.06131	2.06144	4.46947	4.4697	4.57244	4.57324	5.52267
CNT (10,10)	0.574225	0.574228	4.05822	4.05824	4.5203	4.5216	5.77265	6.16681	6.16695

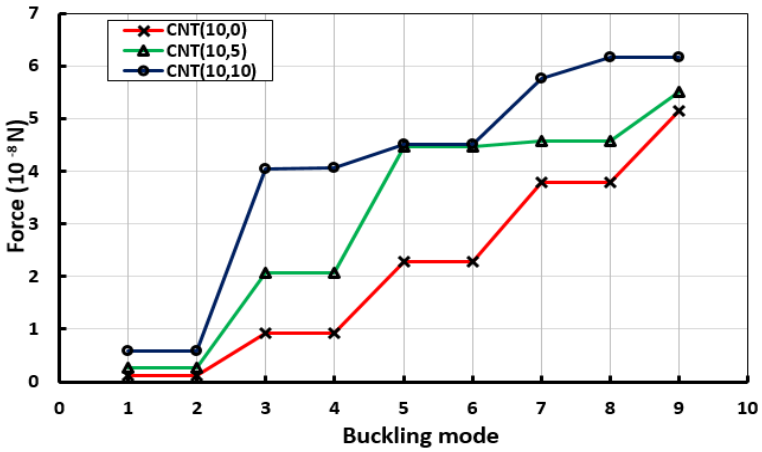

Fig. 6 Buckling Modes and Force (10-8 N) and effects of orientation when CNT length 100 Å

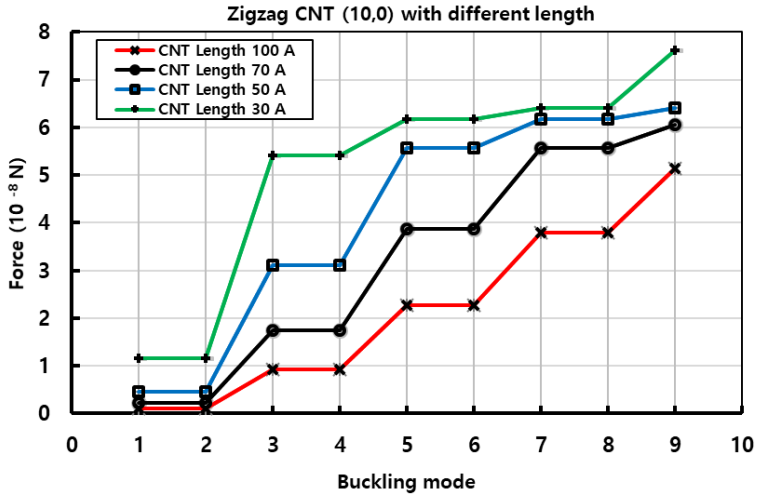

Fig. 7 Effect of NT lengths on the first nine buckling load of zigzag (10, 0) orientations

6. Free vibration behaviors

Through this section, a geometrical structure of SWCNT is generated by nanotube modeler program and then inserted to ANSYS MAPDL environment. Finite element model using 3D beam element with 2 Nodes is proposed to simulate the atomic interaction force. Modal module is selected to evaluate natural frequencies of CNTs structure. Take in Consider three different types of SWCNT, zigzag (10, 0), Chiral (10, 5) and armchair (10, 10), which have the same tube diameter, the same boundary conditions, and the same length of tube. The computed first nine natural frequencies are tabulated in Table 3 and plotted in Fig. 10. It is noted the highest natural frequency is obtained in armchair case, however the smallest one is obtained in zigzag structure. It is also observed that, there are repetition in some modes, that due to a symmetry in geometrical. Fig. 10 shows as the chiral angle increases the frequency increases. Which means that the relationship between them is a proportional relationship. The mode shapes of modal analysis for the three types of SWCNTs are presented in detail in Appendix A.

The effect of CNT length on the first nine natural frequencies for zigzag, chiral and armchair SWCNTs are presented in Figs. 11-13. As shown from three cases, as the length of CNT increases the natural frequencies are decreased. The effect of tube length is more pronounced in small lengths than higher lengths. The length may also affect on the number of repeated frequencies. For example in case of armchair structure, at L = 30 Å the 6th and 7th

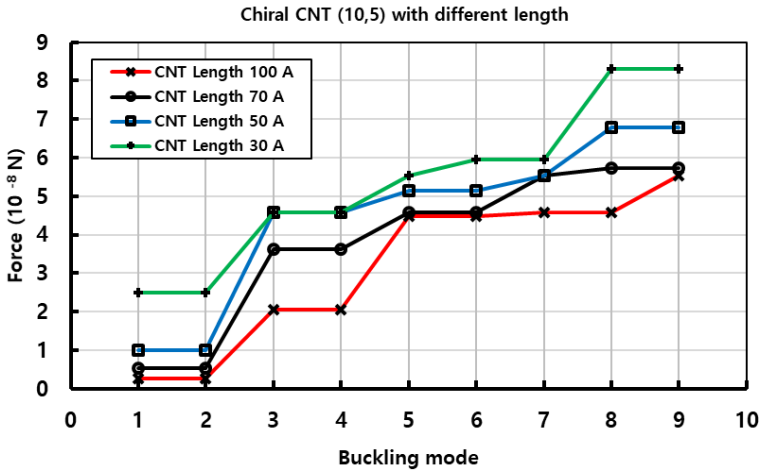

Fig. 8 Effect of NT lengths on the first nine buckling load of chiral (10, 5) orientations

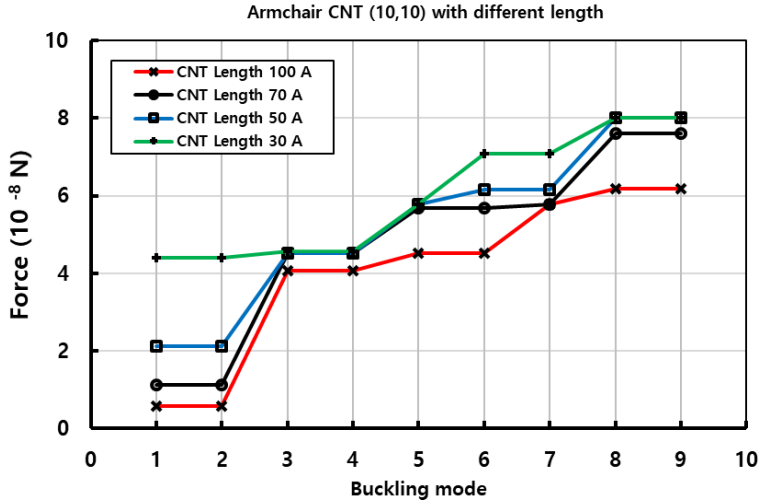

Fig. 9 Effect of NT lengths on the first nine buckling load of armchair (10, 10) orientations

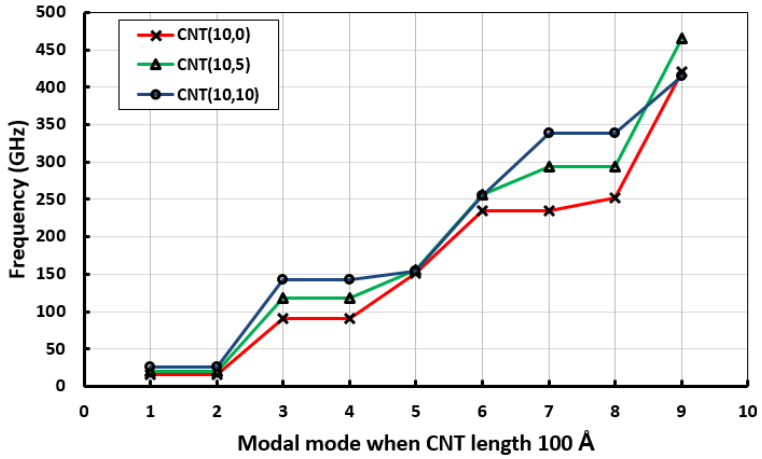

Fig. 10 Modal Modes & frequencies (GHz) for zigzag, chiral and armchair SWCNTs, at LFE = 100 Å

modes are equal, however, at L = 50 Å the 4th to 7th modes (four modes) are equal. So, it can be concluded that, the length of SWCNT has significant effects on both natural frequencies and mode shapes.

7. Conclusions

The main benefit of the proposed method is to saving of computing time, with fair accuracy in estimating the

Table 4 Modal Modes and frequencies (GHz) for zigzag, chiral and armchair SWCNTs, at L_{FE} = 100 Å

Mode	1st	2nd	3rd	4th	5th	6th	7th	8th	9th
CNT (10,0)	15.426	15.426	91.057	91.058	151.59	235.56	235.56	252.44	420.21
CNT (10,5)	20.81	20.811	118.02	118.02	155.15	255.88	293.29	293.3	465.56
CNT (10,10)	26.544	26.544	142.38	142.38	154.18	254.34	338.44	338.44	414.32

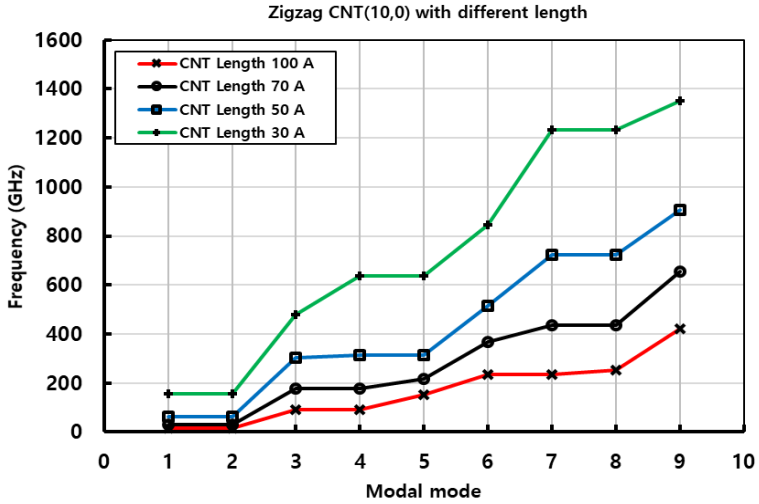

Fig. 11 Effect of NT lengths on the first nine natural frequencies of zigzag (10, 0) orientations

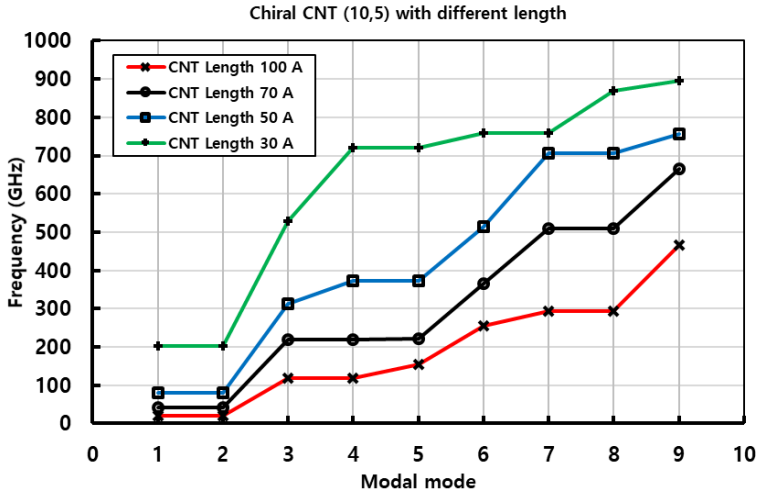

Fig. 12 Effect of NT lengths on the first nine natural frequencies of chiral (10,5) orientations

mechanical properties of the SWCNT when compared to the other methodologies. In this work, we have evaluated the capability of the implemented method to calculate the young's modulus, natural frequency of vibration and the buckling force of carbon nanotubes. The obtained results are compared with data reported by other authors. The main conclusions can be stated as following:

- In static analysis, the equivalent Young's modulus of CNTs is proportional inversely with the length of tubes, and the equivalent Young's modulus of chiral CNT (10, 5) orientation is most significant for a length variation rather zigzag and armchair orientations.
- In buckling analysis, the armchair CNT is more stiffener rather than the other SWCNT orientations, the shorter tube is more stiffener than the longer one, and repeated modes may be observed in some cases.
- In modal analysis, the armchair structure has the highest natural frequencies rather than the other structures at the same length, the natural frequencies is increased by decreasing the tube length.

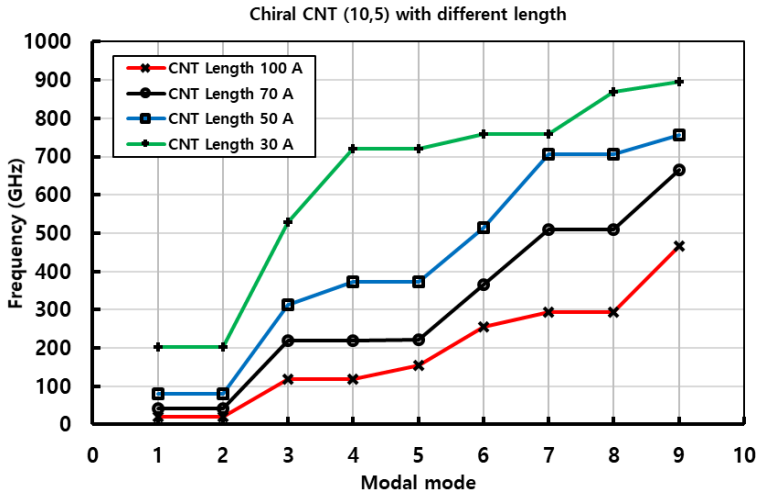

Fig. 13 Effect of NT lengths on the first nine natural frequencies of armchair (10,10) orientations

References

Akgöz, B. and Civalek, Ö. (2016), "Bending analysis of embedded carbon nanotubes resting on an elastic foundation using strain gradient theory", *Acta Astronautica*, **119**, 1-12.

Alessi, R., Favata, A. and Micheletti, A. (2017), "Pressurized CNTs under tension: A finite-deformation lattice model", *Compos. Part B: Eng.*, **115**, 223-235.

Awang, M., Mohammadpour, E. and Muhammad, I.D. (2015), *Finite Element Modeling of Nanotube Structures: Linear and Non-linear Models*, Springer.

Baykasoglu, C., Kirca, M. and Mugan, A. (2013), "Nonlinear failure analysis of carbon nanotubes by using molecular-mechanics based models", *Compos. Part B: Eng.*, **50**, 150-157.

Benguediab, S., Tounsi, A., Zidour, M. and Semmah, A. (2014), "Chirality and scale effects on mechanical buckling properties of zigzag double-walled carbon nanotubes", *Compos. Part B: Eng.*, **57**, 21-24.

Caruntu, D.I. and Luo, L. (2014), "Frequency response of primary resonance of electrostatically actuated CNT cantilevers", *Nonlinear Dyn.*, **78**(3), 1827-1837.

Eberhardt, O. and Wallmersperger, T. (2015), "Energy consistent modified molecular structural mechanics model for the determination of the elastic properties of single wall carbon nanotubes", *Carbon*, **95**, 166-180.

Ebrahimi, F. and Mahmoodi, F. (2018), "Vibration analysis of carbon nanotubes with multiple cracks in thermal environment", *Adv. Nano Res., Int. J.*, **6**(1), 57-80.

Eltaher, M.A. and Agwa, M.A. (2016), "Analysis of size-dependent mechanical properties of CNTs mass sensor using energy equivalent model", *Sens. Actuat. A: Phys.*, **246**, 9-17.

Eltaher, M.A., El-Borgi, S. and Reddy, J.N. (2016a), "Nonlinear analysis of size-dependent and material-dependent nonlocal CNTs", *Compos. Struct.*, **153**, 902-913.

Eltaher, M.A., Agwa, M.A. and Mahmoud, F.F. (2016b), "Nanobeam sensor for measuring a zeptogram mass", *Int. J.of Mech. Mater. Des.*, **12**(2), 211-221.

Eltaher, M.A., Khater, M.E., Park, S., Abdel-Rahman, E. and Yavuz, M. (2016c), "On the static stability of nonlocal nanobeams using higher-order beam theories", *Adv. Nano Res., Int. J.*, **4**(1), 51-64.

Eltaher, M.A., Agwa, M. and Kabeel, A. (2018a), "Vibration Analysis of Material Size-Dependent CNTs Using Energy Equivalent Model", *J. Appl. Computat. Mech.*, **4**(2), 75-86.

Eltaher, M.A., Abdraboh, A.M. and Almitani, K.H. (2018b), "Resonance Frequencies of Size Dependent Perforated Nonlocal Nanobeam", *Microsyst. Technol.*, **24**(9), 3925-3937.

Eltaher, M.A., Kabeel, A.M., Almitani, K.H. and Abdraboh, A.M. (2018c), "Static bending and buckling of perforated nonlocal size-dependent nanobeams", *Microsyst. Technol.*, **24**(12), 4881-4893.

Eltaher, M.A., Mohamed, N., Mohamed, S. and Seddek, L.F. (2019), "Postbuckling of Curved Carbon Nanotubes Using Energy Equivalent Model", *J. Nano Res.* [Accepted]

Emam, S., Eltaher, M., Khater, M. and Abdalla, W. (2018), "Postbuckling and Free Vibration of Multilayer Imperfect Nanobeams under a Pre-Stress Load", *Appl. Sci.*, **8**(11), 2238.

Esbati, A.H. and Irani, S. (2018), "Probabilistic mechanical properties and reliability of carbon nanotubes", *Arch. Civil Mech. Eng.*, **18**(2), 532-545.

Gajbhiye, S.O. and Singh, S.P. (2015), "Vibration characteristics of open-and capped-end single-walled carbon nanotubes using multi-scale analysis technique incorporating Tersoff–Brenner potential", *Acta Mechanica*, **226**(11), 3565-3586.

Genoese, A., Genoese, A., Rizzi, N.L. and Salerno, G. (2017), "On the derivation of the elastic properties of lattice nanostructures: the case of graphene sheets", *Compos. Part B: Eng.*, **115**, 316-329.

Ghadyani, G., Soufeiani, L. and Öchsner, A. (2016), "On the characterization of the elastic properties of asymmetric single-walled carbon nanotubes", *J. Phys. Chem. Solids*, **89**, 62-68.

Ghadyani, G., Soufeiani, L. and Öchsner, A. (2017), "Angle dependence of the shear behaviour of asymmetric carbon nanotubes", *Mater. Des.*, **116**, 136-143.

Haile, J.M. (1992), *Molecular dynamics simulation: elementary methods*, John Wiley & Sons, Inc.

Iijima, S. (1991), "Helical microtubules of graphitic carbon", *Nature*, **354**(6348), 56.

Krishnan, A., Dujardin, E., Ebbesen, T.W., Yianilos, P.N. and Treacy, M.M.J. (1998), "Young's modulus of single-walled nanotubes", *Phys. Rev. B*, **58**(20), 14013.

Kumar, B.R. (2018), "Investigation on mechanical vibration of double-walled carbon nanotubes with inter-tube Van der waals forces", *Adv. Nano Res., Int. J.*, **6**(2), 135-145.

Lee, J.H. and Lee, B.S. (2012), "Modal analysis of carbon nanotubes and nanocones using FEM", *Computat. Mater. Sci.*, **51**(1), 30-42.

Li, C. and Chou, T.W. (2003), "A structural mechanics approach for the analysis of carbon nanotubes", *Int. J. Solids Struct.*, **40**(10), 2487-2499.

Lu, X. and Hu, Z. (2010), "Evaluation of Mechanical Behaviors of Single-Walled Carbon Nanotubes by Finite Element Analysis",

ASME 2010 International Mechanical Engineering Congress and Exposition, *American Society of Mechanical Engineers*, pp. 81-91.

Narendar, S. and Gopalakrishnan, S. (2009), "Nonlocal scale effects on wave propagation in multi-walled carbon nanotubes", *Computat. Mater. Sci.*, **47**(2), 526-538.

Rappé, A.K., Casewit, C.J., Colwell, K.S., Goddard Iii, W.A. and Skiff, W.M. (1992), "UFF, a full periodic table force field for molecular mechanics and molecular dynamics simulations", *J. Am. Chem. Soc.*, **114**(25), 10024-10035.

Shahabodini, A., Ansari, R. and Darvizeh, M. (2018), "Atomistic-continuum modeling of vibrational behavior of carbon nanotubes using the variational differential quadrature method", *Compos. Struct.*, **185**, 728-747.

She, G.L., Yuan, F.G., Ren, Y.R. and Xiao, W.S. (2017a), "On buckling and postbuckling behavior of nanotubes", *Int. J. Eng. Sci.*, **121**, 130-142.

She, G.L., Yuan, F.G. and Ren, Y.R. (2017b), "Nonlinear analysis of bending, thermal buckling and post-buckling for functionally graded tubes by using a refined beam theory", *Compos. Struct.*, **165**, 74-82.

She, G.L., Yuan, F.G., Ren, Y.R., Liu, H.B. and Xiao, W.S. (2018a), "Nonlinear bending and vibration analysis of functionally graded porous tubes via a nonlocal strain gradient theory", *Compos. Struct.*, **203**, 614-623.

She, G.L., Ren, Y.R., Yuan, F.G. and Xiao, W.S. (2018b), "On vibrations of porous nanotubes", *Int. J. Eng. Sci.*, **125**, 23-35.

She, G.L., Yuan, F.G., Karami, B., Ren, Y.R. and Xiao, W.S. (2019), "On nonlinear bending behavior of fg porous curved nanotubes", *Int. J. Eng. Sci.*, **135**, 58-74.

Shokrieh, M.M. and Rafiee, R. (2010), "Prediction of Young's modulus of graphene sheets and carbon nanotubes using nanoscale continuum mechanics approach", *Mater. Des.*, **31**(2), 790-795.

Vila, J., Fernández-Sáez, J. and Zaera, R. (2018), "Reproducing the nonlinear dynamic behavior of a structured beam with a generalized continuum model", *J. Sound Vib.*, **420**, 296-314.

Yuan, X. and Wang, Y. (2018), "Radial deformation of single-walled carbon nanotubes adhered to solid substrates and variations of energy: atomistic simulations and continuum analysis", *Int. J. Solids Struct.*

Wu, Y., Zhang, X., Leung, A.Y.T. and Zhong, W. (2006), "An energy-equivalent model on studying the mechanical properties of single-walled carbon nanotubes", *Thin-Wall. Struct.*, **44**(6), 667-676.

Zuberi, M.J.S. and Esat, V. (2016), "Evaluating the effects of size and chirality on the mechanical properties of single-walled carbon nanotubes through equivalent-continuum modelling", *Proceedings of the Institution of Mechanical Engineers*, *Part L*: *Journal of Materials*: *Design and Applications*, **230**(5), 913-926.

CC